CSIRO PUBLISHING

Exploration Geophysics
http://dx.doi.org/10.1071/EG16014

Joint inversions of two VTEM surveys using quasi-3D TDEM and 3D magnetic inversion algorithms

Vlad Kaminski[1,3] Domenico Di Massa[2] Andrea Viezzoli[1]

[1]Aarhus Geophysics, Aps, Lollandsgade 52, Aarhus, DK-8000, Denmark.
[2]Department of Earth, Environment and Resources Sciences, University of Naples Federico II, Largo San Marcellino 10, Naples 80138, Italy.
[3]Corresponding author. Email: vlad.kaminski@aarhusgeo.com

Abstract. In the current paper, we present results of a joint quasi-three-dimensional (quasi-3D) inversion of two versatile time domain electromagnetic (VTEM) datasets, as well as a joint 3D inversion of associated aeromagnetic datasets, from two surveys flown six years apart from one another (2007 and 2013) over a volcanogenic massive sulphide gold (VMS-Au) prospect in northern Ontario, Canada. The time domain electromagnetic (TDEM) data were inverted jointly using the spatially constrained inversion (SCI) approach. In order to increase the coherency in the model space, a calibration parameter was added. This was followed by a joint inversion of the total magnetic intensity (TMI) data extracted from the two surveys. The results of the inversions have been studied and matched with the known geology, adding some new valuable information to the ongoing mineral exploration initiative.

Key words: airborne EM, inversion, magnetics, TDEM, VMS.

Received 7 February 2016, accepted 31 March 2016, published online 30 May 2016

Introduction

Two versatile time domain electromagnetic (VTEM) surveys were flown over the Broken Evil volcanogenic massive sulphide gold (VMS-Au) prospect in northern Ontario, Canada (Figure 1). Both surveys measured total magnetic intensity (TMI), as well as time domain electromagnetic (TDEM) response. The first survey was flown at 200 m spacing in 2007, followed by another survey with a different VTEM system flown at 200 m spacing in 2013 (Figure 2). Together, the surveys create an area covered by joint VTEM survey with 100 m line spacing, subject for joint inversion. The two VTEM systems used on the project had different dipole moments, waveform shapes and receiver times. From an instrumental point of view, they represent two completely distinct datasets.

First, the TMI data were extracted from the two datasets, inverted separately, then jointly, using the Mag3D code developed at University of British Columbia Geophysical Inversion Facility (UBC-GIF) (Li and Oldenburg, 1996). This was followed up by additional TDEM data post-processing and preparation for spatially constrained inversion (SCI), a quasi-three-dimensional (quasi-3D) inversion approach (Viezzoli et al., 2008) using 'AarhusINV' (Kirkegaard and Auken, 2015).

Geology

The Broken Evil prospect lies in the Abitibi Greenstone Belt, in the eastern part of Superior Province and is underlain by intermediate, mafic and ultramafic metavolcanics as well as pyroclastics and metasediments (Figure 3). These early Precambrian units have been intruded by several metamorphosed mafic and ultramafic bodies. The Abitibi terrane hosts some of the richest mineral deposits of the Superior Province, including the giant Kidd Creek VMS deposit (Hannington et al., 1999) and the large gold camps of Ontario and Quebec (Robert and Poulsen, 1997).

Both historic and new drilling data are available for the study area. The most recent drilling program took place in 2011, initialised by Promiseland Exploration Ltd of Vancouver, following the interpretation of a ground frequency domain (electromagnetic) EM geophysical survey of the area (Kaminski et al., 2011). According to this interpretation, an anomalous conductive zone was delineated and drill-tested as a potential VMS target. The 2011 drilling program revealed a 21 m thick VMS zone with disseminated to massive mineralised intervals starting at 82 m below surface. Four types of sulphide minerals were recovered from the core samples, including pyrite, pyrhotite, chalcopyrite and sphalerite, which are typical of a VMS system.

There is an ongoing exploration program in the area; it is expected that other VMS deposits will generate strong conductive and chargeable anomalies, which may or may not be magnetic (e.g. the Kidd Creek deposit is non-magnetic). Within the extent of this ongoing exploration survey are two main targets that are the subject of the current study.

AarhusINV SCI inversions

Two VTEM surveys (2007 and 2013) were carried out over the Broken Evil prospect. Although each individual VTEM survey was flown with 200 m line spacing, together the surveys create an area covered by 100 m line spacing (Figure 2). The VTEM systems used for the surveys have different transmitter and receiver times, as well as off-time decay-sampling (Figure 4). Effectively, the 2007 VTEM is a 'short-pulse' system with higher peak current (and dipole moment), but shorter on-time

Fig. 1. The location of the Broken Evil prospect in northern Ontario, Canada.

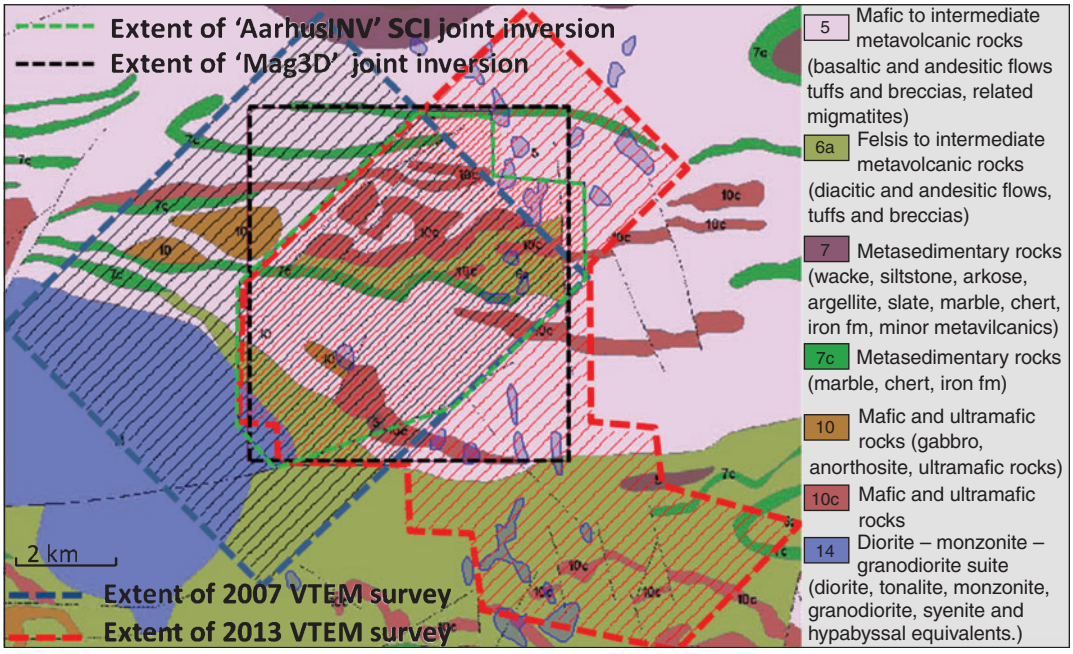

Fig. 2. The extent of the 2007 and 2013 VTEM surveys and joint SCI and Mag3D inversions plotted over bedrock geology of the study area (bedrock geology adapted from Geological Survey of Ontario, 2011).

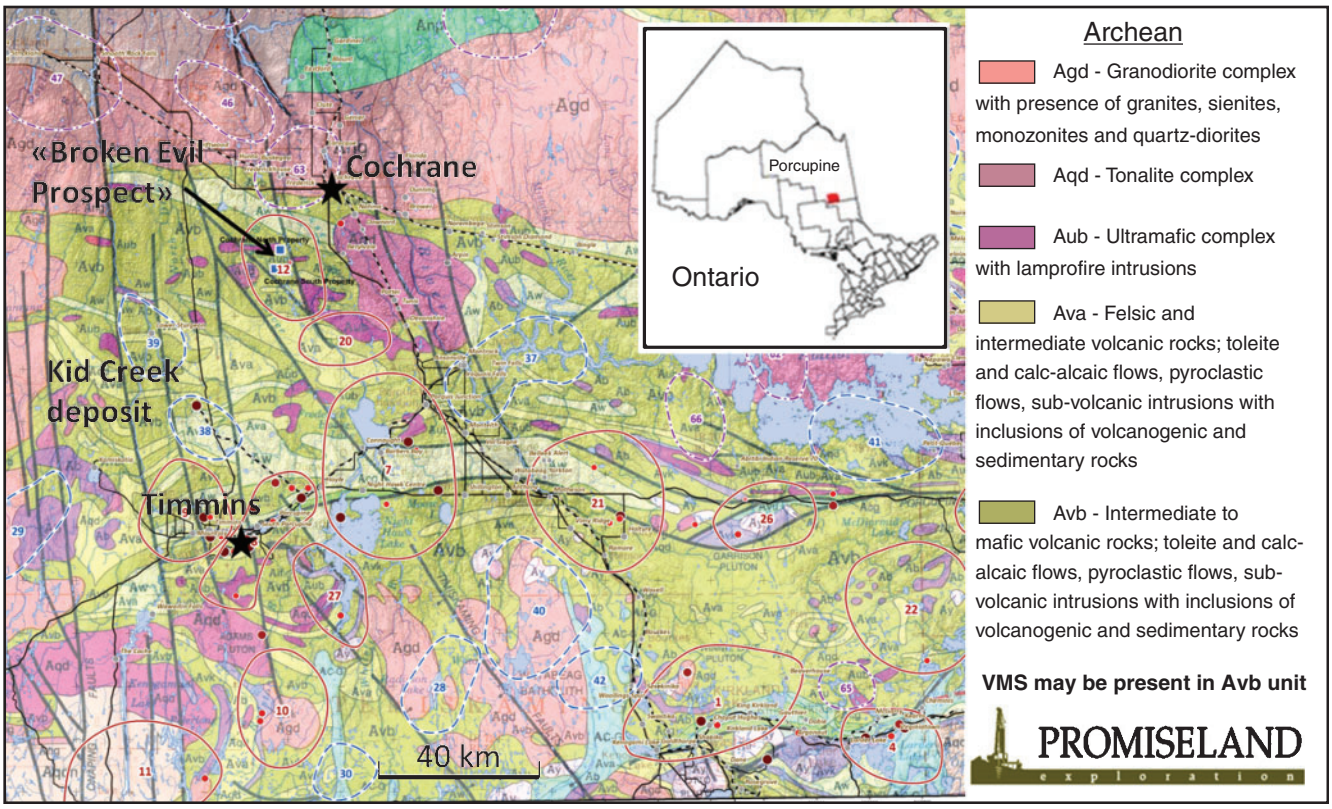

Fig. 3. Regional geological setting.

pulse (4.3 ms), while the 2013 system allows longer on-time pulse (7.12 ms), but lower dipole moment. Both systems share similar off-time ranges (from 100 μ to 10000 μ); however, the off-time sampling intervals and noise levels in the data are also different, which makes joint inversion effectively similar to jointly inverting data from two completely different airborne systems.

An attempt was made to jointly invert the data using two description files. The EM data inversion of the two datasets was carried out in a joint approach using the SCI algorithm (Viezzoli et al., 2008). The global data misfit, normalised by the standard deviations, is satisfactory (below 3), but the results appear to be affected by striping parallel to the flight lines in correspondence to the different surveys. The latter can be attributed to imperfections in calibration between the two VTEM datasets or possibly imperfections in altitude measurements in 2007, which was significantly improved by 2013. It is, however, possible to minimise this effect by adjusting the parameters of the system transfer functions (Sapia et al., 2014).

The imperfections in calibration of the two VTEM systems are manifested as shifts in amplitude between measurements performed over the same sounding position. There is a very small area within the extent of the SCI inversion area where the 2007 flight lines overlap with the 2013 flight lines (Figure 5). This area was used to study the calibration of the two systems relative to one another. Dozens of coincident transients were assessed. Those which fell within areas of strong three-dimensional (3D) variations were discarded, and the final calibration factor for the entire survey was derived from the others.

Currently, it is impossible to obtain absolute calibration of the two VTEM systems used in the study; therefore, the systems were calibrated to one another. The voltage data from the 2013 VTEM has been shifted by a constant in order to make the transient amplitudes comparable to those measured by the 2007 VTEM system.

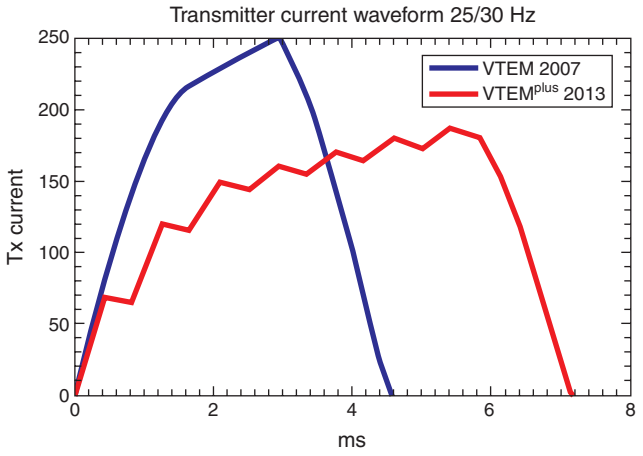

Fig. 4. Comparison of 2007 (short-pulse) and 2013 (long-pulse) VTEM waveforms.

After applying the amplitude shift to the 2013 VTEM data, the data were incorporated in a new joint inversion attempt. The results of the two inversions (before and after the recalibration) plotted against each other are shown in Figure 6.

As it can be seen, the recalibration procedure provides improved model output (Figure 6*b*) by significantly reducing the striping artefacts without increasing the data misfit. The results of the SCI inversion have been plotted as a series of depths slices over the bedrock geology (Figure 7).

The two areas circled with dashed red lines are the main exploration targets selected for the drilling program. These targets are situated in a favourable geological setting. Zone

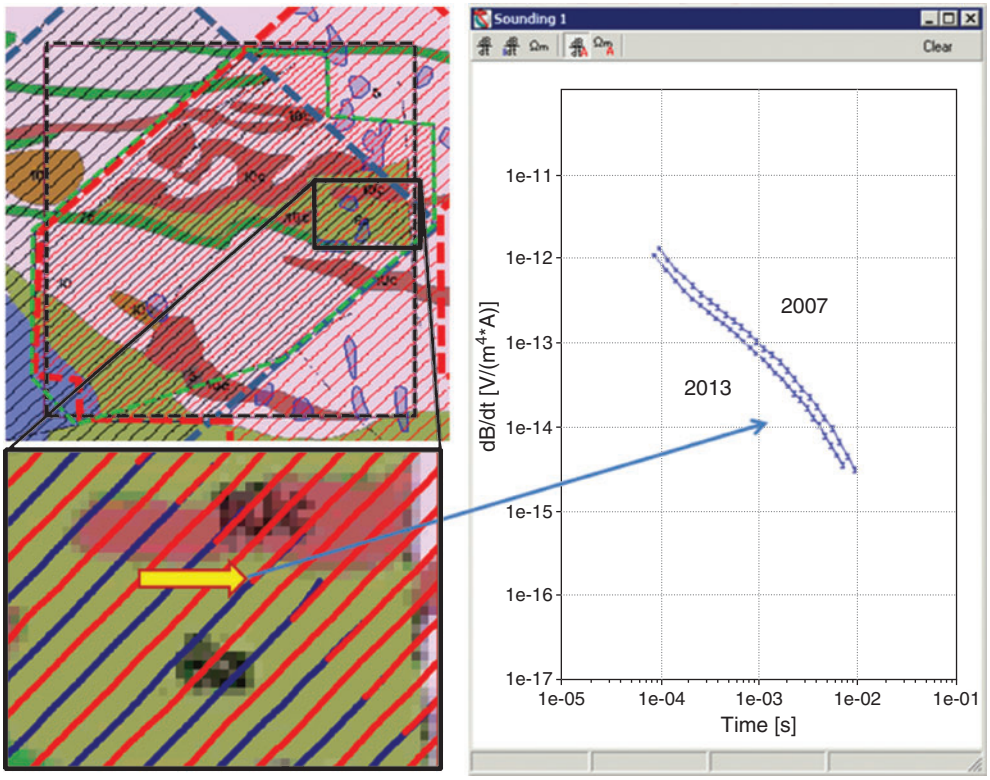

Fig. 5. Location of the sounding with overlapping VTEM flight lines used for recalibration of the VTEM systems for joint SCI inversion. Notice the obvious constant amplitude shift between the two transients (both normalised by their moment).

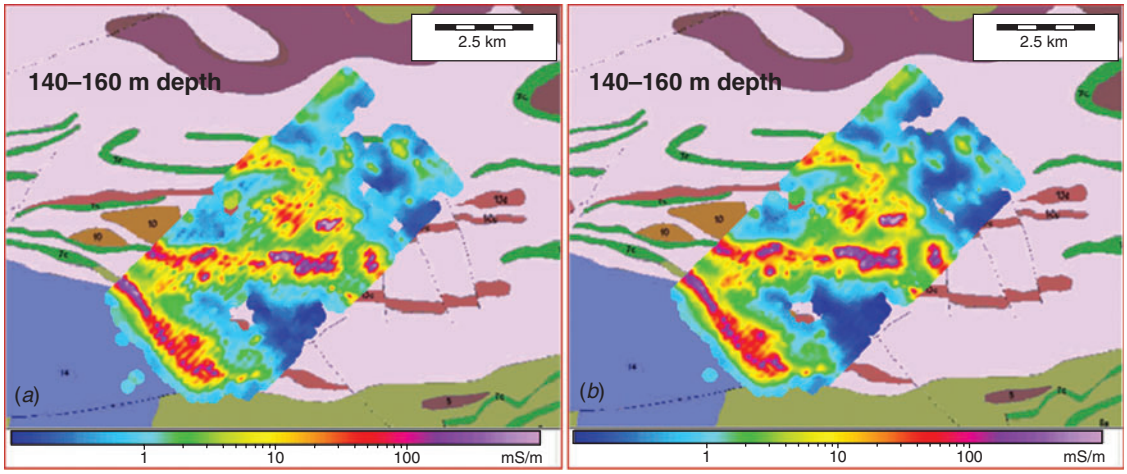

Fig. 6. (*a*) Slice of recovered electrical resistivity at 160 m below surface before applying the constant amplitude shift. (*b*) Depth slice of recovered electrical resistivity at 160 m below surface after applying the constant shift to VTEM 2013 voltage data.

number 1 is situated within 100 m to DH-02, which intersected a 22 m thick semi-massive mineralised zone at depth of 82 m during the 2011 exploration program. As can be seen in Figure 7, both zones are associated with very high values of electrical conductivity, which may be consistent with massive sulphidisation.

3D magnetic inversion

The 3D magnetic inversion was carried out using Mag3D, the inversion code developed at UBC-GIF (Li and Oldenburg, 1996). First, the 2007 data were extracted and corrected using the International Geomagnetic Reference Field (IGRF), then the inversion was performed on a coarse mesh (134 × 147 × 92 cells in X, Y and Z directions, respectively), with each cell measuring 50 × 50 m horizontally and ranging from 10 to 100 m vertically. A similar procedure was done for the 2013 TMI data over an identical mesh. Then the datasets were combined together and levelled in order to adjust the different levels after the IGRF corrections.

The parameters of the normal field were also adjusted accordingly; the final inversion was performed over a total of 19 593 data stations over a refined mesh (258 × 282 × 93 cells in X, Y and Z directions, respectively) with each cell measuring

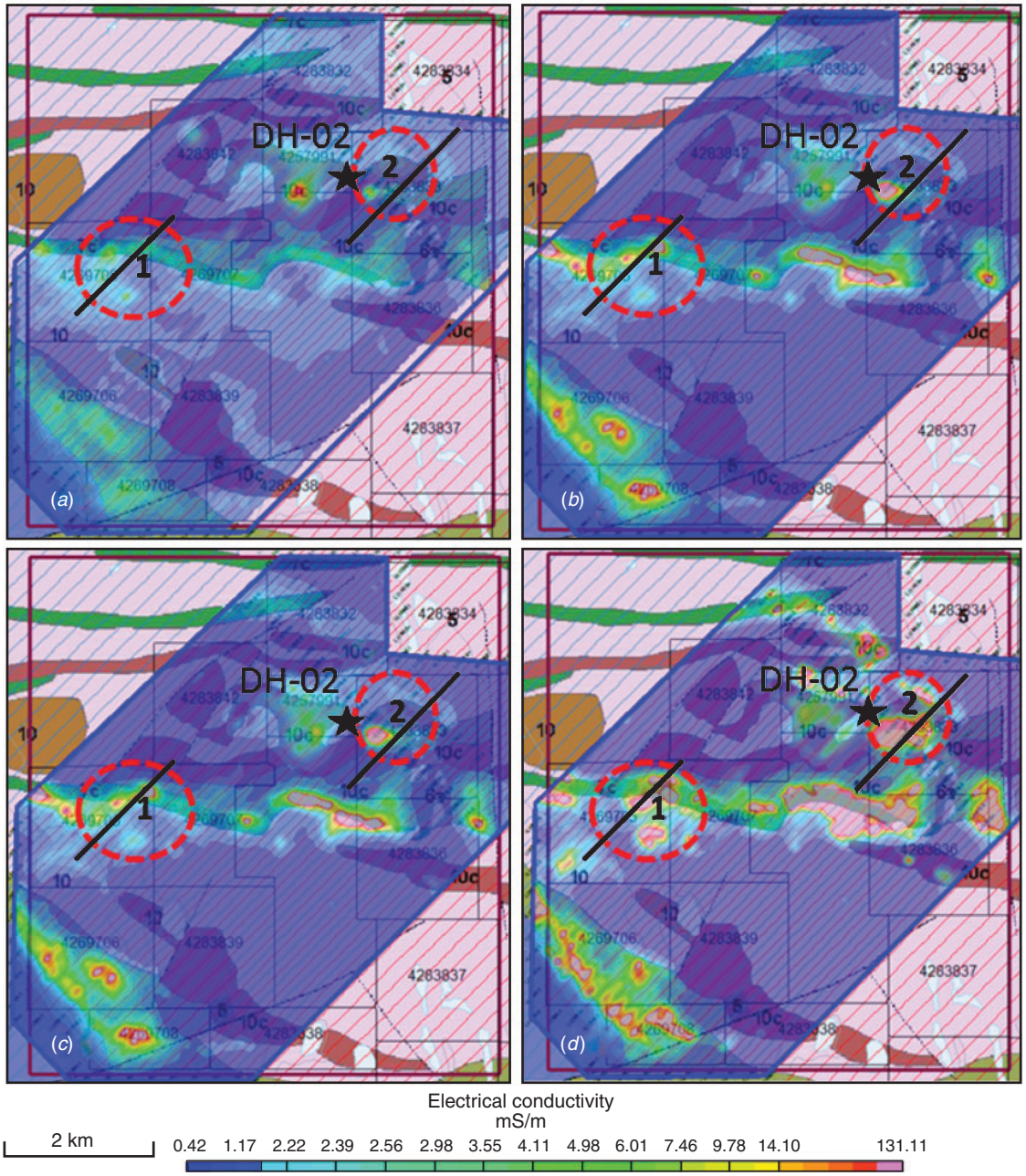

Fig. 7. Results of joint SCI inversion of recalibrated VTEM data plotted over bedrock geology at different elevation (depth) slices: (*a*) 230 m level; (*b*) 180 m level; (*c*) 120 m level; (*d*) 65 m level. Note the thick black line sections corresponding to the cross-section locations shown in Figures 10 and 11. The black star marks DH-02 (drillhole number 2) from the 2011 drilling program.

25 m in X and Y directions for enhanced spatial resolution. A padding distance of 1.05 km in every direction was allowed. Magnetic susceptibility was recovered to depths of more than 2500 m. The data fit for each individual TMI inversion was better than for the combined dataset (5 nT against 10 nT); however, the data fit on the joint inversion is good (Figure 8), and the resulting susceptibility models were very similar.

The results of the 3D magnetic inversion are shown in Figure 9, plotted as a series of magnetic susceptibility depth slices positioned over bedrock geology (consistent with depth slices of electrical conductivity shown in Figure 7). The two exploration targets are circled in a red dashed line and numbered. Although the interpreted conductive plates are not shown as magnetic units, in area 2 the target is adjacent to a highly magnetic structure (> 0.25 SI units), which is interpreted to be a peridotite complex.

Discussion

The results of the quasi-3D SCI and 3D magnetic inversions were plotted against some earlier modelling results acquired over two current exploration targets using resistivity depth imagery (RDI) transformations (Meju, 1998) and plate modelling. Two areas were of particular interest as they are subject to current mineral exploration and are classified as priority drill targets. Figures 10 and 11 show these areas in cross-sections with inclusion of the magnetic susceptibilities recovered from the Mag3D inversions. In plain view, the corresponding parts of flight lines can be seen in Figures 7 and 9 (shown as thicker black

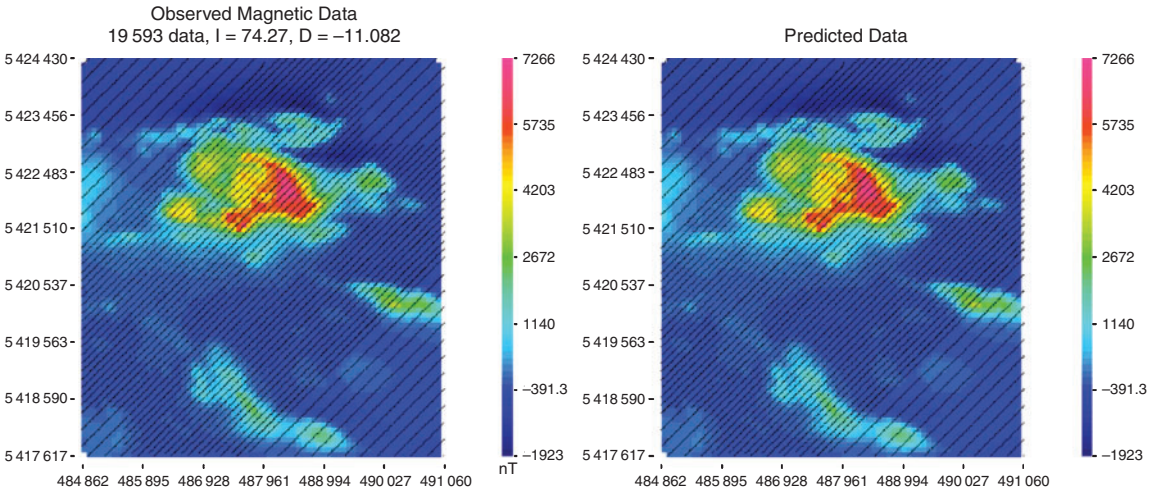

Fig. 8. Data fit for the joint Mag3D inversion.

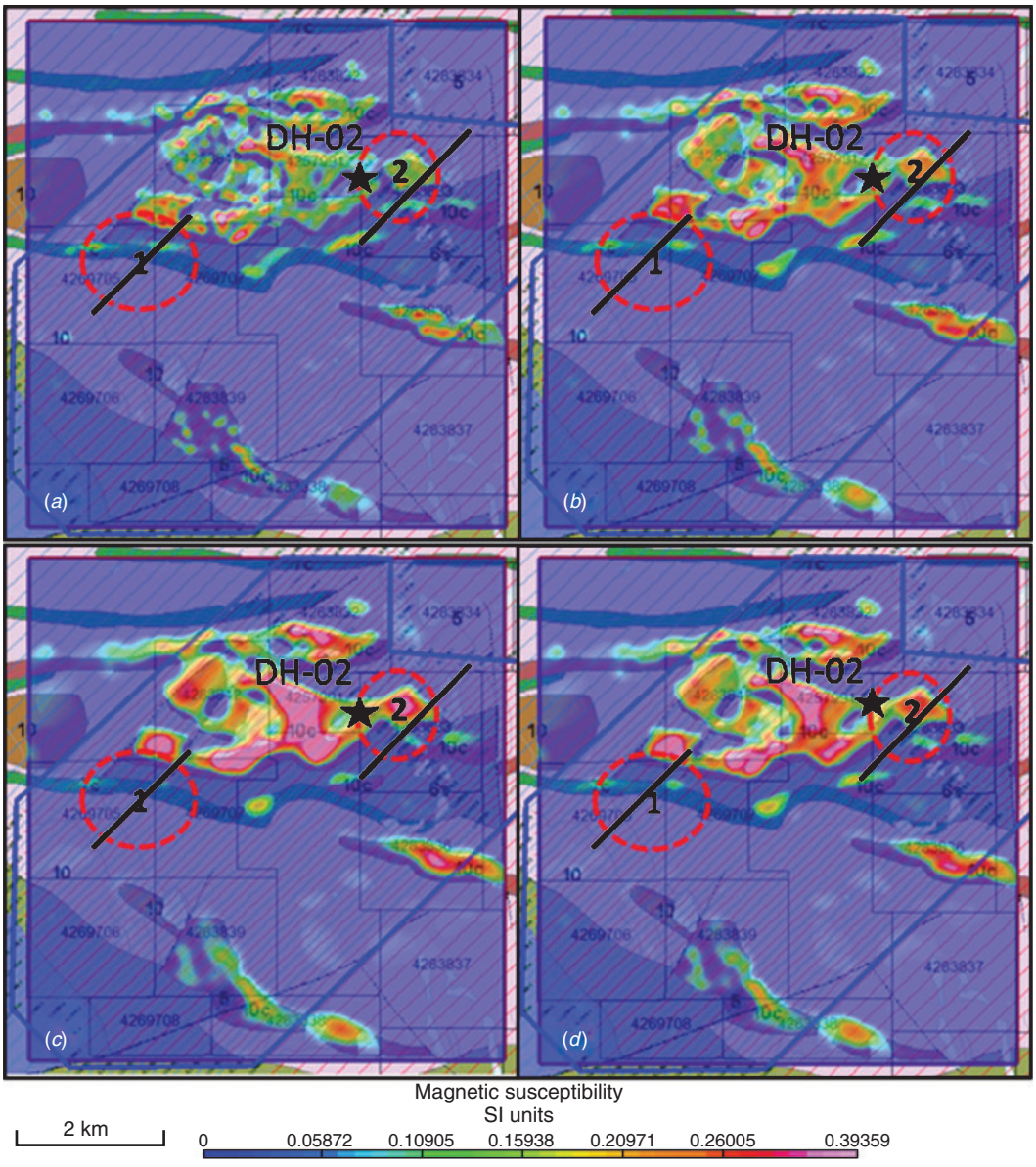

Fig. 9. Mag3D inversion results plotted as depth slices of absolute elevation: (*a*) 230 m level; (*b*) 180 m level; (*c*) 120 m level; (*d*) 65 m level. Note the thick black line sections corresponding to the cross-section locations shown in Figures 10 and 11. The black star marks DH-02 (drillhole number 2) from the 2011 drilling program.

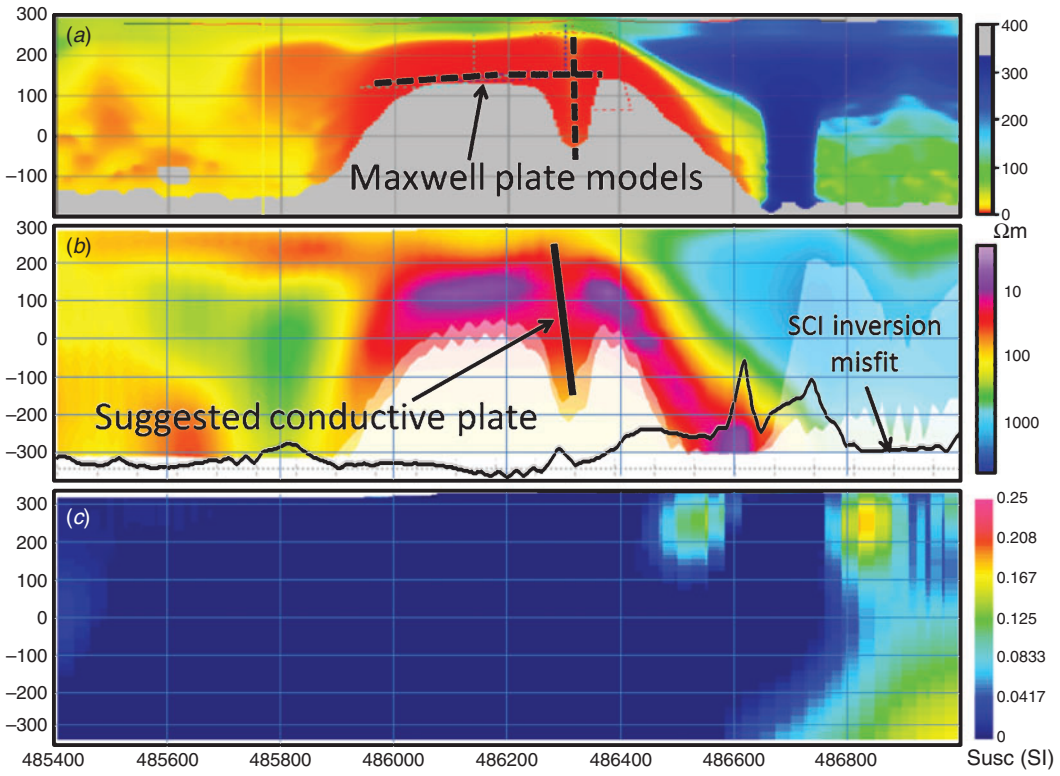

Fig. 10. Section from VTEM line 1080 (2013 survey): (*a*) results of RDI transforms and Maxwell plate modelling; (*b*) results of SCI inversion; (*c*) results of Mag3D inversion. This cross-section is shown in plain view on Figures 7 and 9 (area 1).

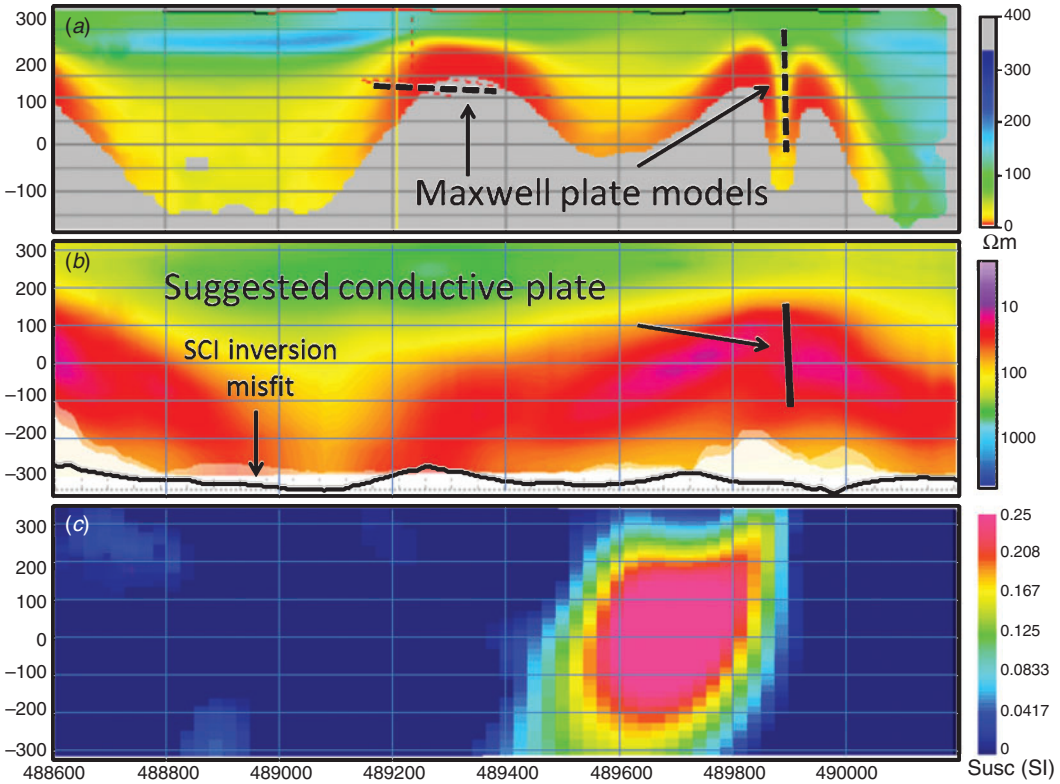

Fig. 11. VTEM line 1240 (2013 survey), target 2: (*a*) results of RDI transforms and Maxwell plate modelling; (*b*) results of SCI inversion; (*c*) results of Mag3D inversion. This cross-section is shown in plain view on Figures 7 and 9 (area 2).

line sections). In the TDEM inversions and transforms, 2D or 3D effects are evident. Using a one-dimensional (1D) forward modelling kernel, which is used in the SCI inversion program, the obtained models are influenced by these 3D effects that result in artefacts known as 'pantlegs' (Christiansen et al., 2009: pp. 179–226) in the inverse models.

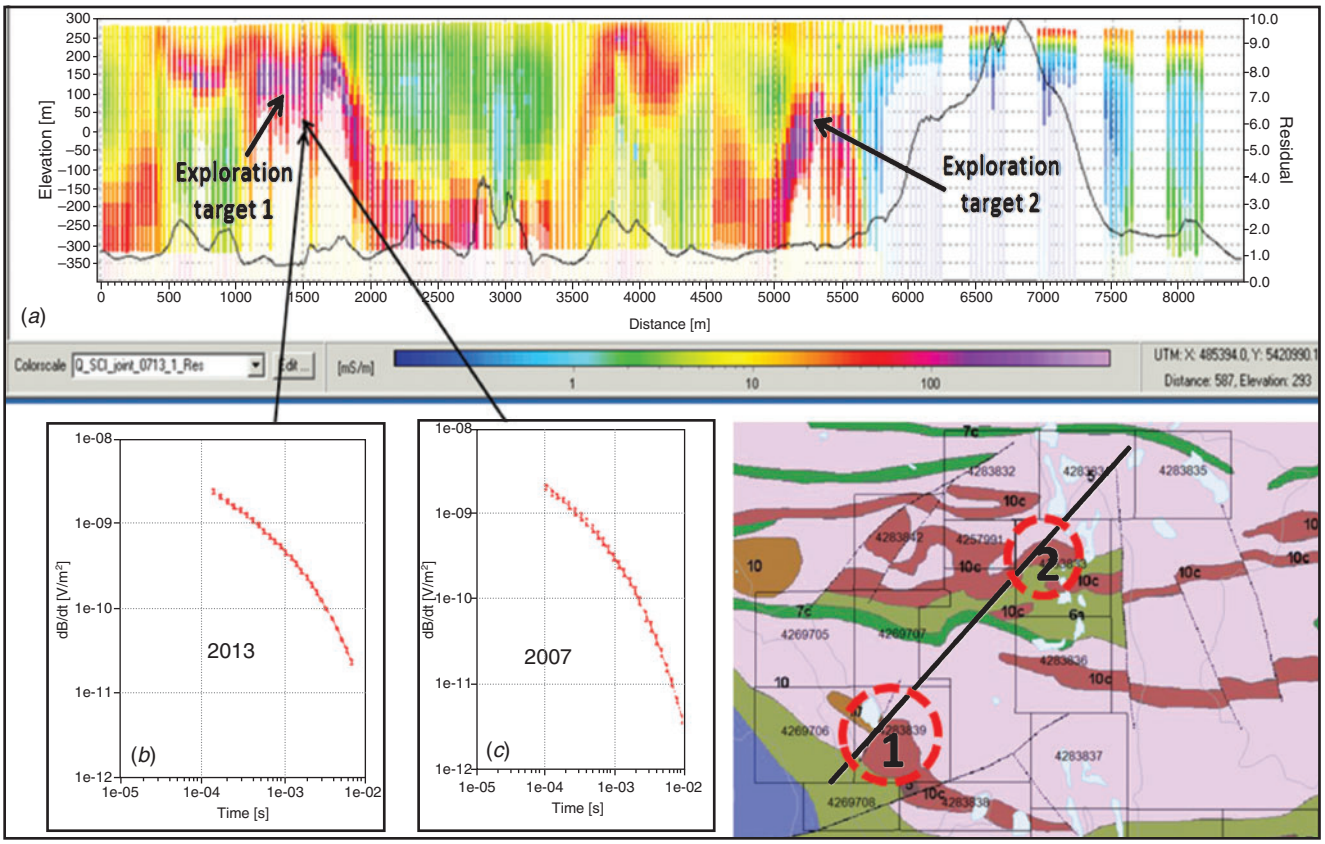

Fig. 12. Electrical profile over two priority exploration targets: (*a*) geo-electrical section based on joint SCI inversion results; (*b*) data fit for a selected 2013 transient; (*c*) data fit for selected 2007 transient.

These 'pantlegs' are interpreted to be representative of thin steeply dipping conductors. This is further supported by the 3D magnetic inversion, which also suggests subvertically dipping structures. Figure 12 shows an interpolated cross-section crossing both exploration targets from south-west to north-east.

The conductivity anomalies are associated with metasedimentary units as well as felsic and intermediate metavolcanic rocks and ultramafic rocks (Figure 2). There appears to be strong VMS potential within these rock types in the area. The targets remain undrilled; therefore, the suggested interpretation is pending confirmation.

Conclusions

This study shows a successful practical attempt to jointly invert two VTEM datasets collected six years apart from one another and with significantly different waveforms and measurement times. The SCI inversion has produced a common 3D resistivity model, which fits both datasets to an acceptable misfit. Application of a calibration factor to one of the datasets yielded higher spatial coherence in the model space. Similarly, we were able to fit the TMI data to desired misfit, producing a single 3D magnetic susceptibility model. The results appear to be quite interpretable geologically and consistent with previous interpretations of these datasets, but with enhanced spatial resolution due to closer line spacing (100 m in combined dataset as opposed to 200 m in each of the individual sets). The advantage of obtaining one single 3D model fitting all data at once rather than two models (one fitting each dataset) is obvious in terms of overall robustness of the geophysical results and of any of the subsequent modelling.

Acknowledgements

The authors would like to thank Promiseland Exploration Ltd for providing the VTEM data, as well as Geotech Ltd for their contribution to better understanding of VTEM data and for their input in assessing the results of inversions.

References

Christiansen, A. V., Auken, E., and Sørensen, K., 2009, *The transient electromagnetic method in groundwater geophysics*: Springer.

Geological Survey of Ontario, 2011, Preliminary map, 1 : 250000. Available at: http://www.geologyontario.mndm.gov.on.ca/

Hannington, M. D., Barrie, C. T., and Bleeker, W., 1999, The giant Kidd Creek volcanogenic massive sulfide deposit, western Abitibi Subprovince, Canada, *in* M. D. Hannington, and C. T. Barrie, eds., *The giant Kidd Creek volcanogenic massive sulfide deposit, Western Abitibi Subprovince, Canada*: Economic Geology Monograph **10**, 1–30.

Kaminski, V., Oldenburg, D., and Prikhodko, A., 2011, Using ERA low frequency E-field profiling and UBC 3D frequency-domain inversion to delineate and discover a mineralized zone in Porcupine district, Ontario: SEG Technical Program, Expanded Abstracts, 1262–1266.

Kirkegaard, C., and Auken, E., 2015, A parallel, scalable and memory efficient inversion code for very large-scale airborne electromagnetics surveys: *Geophysical Prospecting*, **63**, 495–507. doi:10.1111/1365-2478.12200

Li, Y., and Oldenburg, D., 1996, 3D inversion of magnetic data: *Geophysics*, **61**, 394–408. doi:10.1190/1.1443968

Meju, M., 1998, A simple method of transient electromagnetic data analysis: *Geophysics*, **63**, 405–410. doi:10.1190/1.1444340

Robert, F., and Poulsen, K. H., 1997, World-class Archaean gold deposits in Canada: an overview: *Australian Journal of Earth Sciences*, **44**, 329–351. doi:10.1080/08120099708728316

Sapia, V., Oldenborger, G. A., Viezzoli, A., and Marchetti, M., 2014, Incorporating ancillary data into the inversion of airborne time-domain electromagnetic data for hydrogeological applications: *Applied Geophysics*, **104**, 35–43. doi:10.1016/j.jappgeo.2014.02.009

Viezzoli, A., Christiansen, A. V., Auken, E., and Sørensen, K., 2008, Quasi-3D modeling of airborne TEM data by spatially constrained inversion: *Geophysics*, **73**, F105–F113. doi:10.1190/1.2895521